



A Chaotic Clifford Attacker Map-based Image Encryption in Double Random Phase Encoding

Sahil Kalra ^{a*}, Vikash Siwach ^a, Poonam Redhu ^b and Vandna ^c

^a Department of Mathematics and Statistics, College of Basic Sciences and Humanities, Chaudhary Charan Singh Haryana Agricultural University, Hisar - 125004, Haryana, India.

^b Department of Mathematics, Maharshi Dayanand University, Rohtak, Haryana, India.

^c Department of Mathematics, Manohar Memorial College, Fatehabad, Haryana, India.

Authors' contributions

This work was carried out in collaboration among all authors. All authors read and approved the final manuscript.

Article Information

DOI: 10.9734/CJAST/2022/v41i383978

Open Peer Review History:

This journal follows the Advanced Open Peer Review policy. Identity of the Reviewers, Editor(s) and additional Reviewers, peer review comments, different versions of the manuscript, comments of the editors, etc are available here: <https://www.sdiarticle5.com/review-history/93025>

Original Research Article

Received 22 August 2022
Accepted 25 October 2022
Published 31 October 2022

ABSTRACT

Encryption is the most useful technique used for the security of data during storage and transmission. A well-known encryption scheme called Double Random Phase encoding was introduced by Refregier and Javidi. But due to its linear nature, this scheme has been proven vulnerable against Known plaintext and chosen plaintext attacks. Here in this paper, we propose a chaotic map-based nonlinear encryption scheme that enhances the security of the DRPE encryption scheme for images. Clifford attacker is a non-linear chaotic map that has four parameters and two initial values. This map is highly sensitive to these values. Therefore, these parameters and initial values work as extra secret keys. MATLAB simulation shows that the proposed technique enhances the security level of the DRPE and at the same time has a better immunity to noise and occlusion attacks.

Keywords: Encryption; chaotic map; DRPE; Clifford attacker map; sensitivity analysis.

1. INTRODUCTION

In the current era of technology, the problem of the security of data has augmented. Most of the data transmitted via the internet are in the form of photos and videos. We always want to secure our data during its transmission. Even though there are a variety of security features available, image encryption is particularly important for protecting data in the form of images. Advanced encryption standards (AES) and data encryption standards (DES) are two types of digital image encryption algorithms that have been created [1,2]. However, digital encryption solutions have drawbacks such as computing complexity, time consumption, and sequence algorithm. These methods may be breakable once high-performance computing devices become available. To overcome these limitations, people all over the world are becoming increasingly interested in optical cryptosystems. As these optical cryptosystems have inherent properties such as large information capacity, parallel processing, low computational complexity, multiple parameters such as wavelength amplitude focal length, which also serves as an extra encryption key, and high speed.

After an optical encryption scheme based on double random phase encoding proposed in [3], optical technologies have become increasingly attractive for the security of information. Random phase masks are employed in both the spatial and Fourier domains to encrypt an input image to stationary white noise in DRPE-based optical schemes. [4,5] demonstrated that the Double Random Phase Encryption technique is resistant to noise introduced into the encrypted image. DRPE-based schemes were further investigated and enhanced by many researchers using different transformations namely fractional Fourier, Fresnel domain, and Hartley transformation [6-9]. Further, it was found that all these DRPE-based schemes are symmetric and linear. Due to symmetric and linear, cryptanalysis of these schemes shows that these schemes are vulnerable to some attacks [10-12]. To resist these attacks, a nonlinear chaotic map-based encryption scheme was introduced [13-17]. Elshamy et al. [14] developed a system based on the use of a chaotic baker map as a preprocessing layer to allow for pixel randomization, followed by the use of a double random phase encoding layer. To improve the security of the DRPE Scheme, Sharma et al. [16] adopted the 3-D Lorenz system in the Fourier domain. Many other encryption schemes using

chaotic maps in different ways to make more secure encryption schemes are discussed in [18-21].

Chaotic maps have a wide range of applications in the field of cryptography due to their qualities such as uncertainty in prediction, the sensitivity of parameter and beginning values, unpredictable behavior, and many more, Sensitivity of the parameter is a very strong property of chaotic maps, therefore, these parameters can be used as encryption keys. Clifford attacker map is one of the most sensitive chaotic maps which is used in [22,23]. In this paper, we will also use this map for pixel randomization.

In section 2, we discuss the methodology used. The strength of the encryption scheme and robustness against different attacks are discussed in section 3. The paper is concluded in sections 4 followed by the references.

2. MATERIALS AND METHODS

2.1 Double Random Phase Encoding

The DRPE approach proposed in [3] is based on altering an image's intensity distribution. This is accomplished by the use of random phase masks, which result in an encrypted image. We can't decrypt the encrypted image into the original image without any information about the alteration. The input image is first multiplied by a random phase mask (RPM1), after that it is subjected to a Fourier transformation. In the Fourier domain, another random phase mask (RPM2) is applied to the converted image, followed by a second Fourier transformation, yielding into the encrypted image.

Here RPM1 and RPM2 are defined as follows:

$$RPM1 = \exp(2\pi im(x, y))$$

$$RPM2 = \exp(2\pi in(x, y))$$

Mathematically, we can write this encryption process as:

$$e(x, y) = FT(FT(I(x, y) * RPM1) * RPM2)$$

Where $I(x, y)$ is the input image and RPM1 and RPM2 are random phase mask 1 and random phase mask 2 respectively. In the decryption procedure, the inverse Fourier transformation of

an encrypted image is multiplied by the complex conjugate of the second random phase mask and then the image is subjected to another inverse Fourier transformation. As a result, the output is

$$IFT \left(IFT(e(x,y)) * abs(RPM2) \right) = I(x,y) * RPM1$$

whose absolute value turns out to be the decrypted image $I(x,y)$.

The elements which are used to encrypt an input image are called encryption keys and the elements which are used to decrypt the encrypted image are called decryption keys. Here RPM1 and RPM2 are encryption keys. The complex conjugate of RPM2 serves as the decryption key,

Diagrammatically, the whole process of encryption and decryptions is shown below:

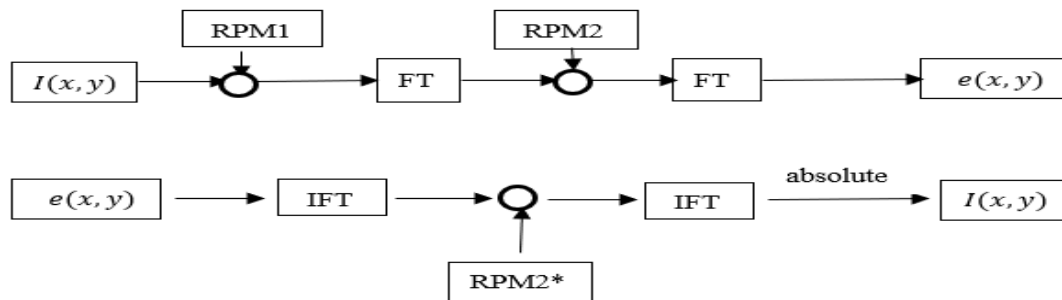


Fig. 1. Encryption and decryption process of DRPE

2.2 Clifford Attacker Map

Clifford attacker map is a two-dimensional chaotic map that generates a sequence of random numbers. This map is used as a tool to enhance the security of the encryption scheme by pixel randomization of the transformed image in the Fourier domain. Mathematically, this map is written as:

$$x_{n+1} = \sin(ay_n) + c \cos(ax_n)$$

$$y_{n+1} = \sin(bx_n) + d \cos(by_n)$$

where a, b, c, d are the parameters and x_0, y_0 are the initial values of this map. These parameters and initial values of this map are highly sensitive. As a result, these values serve as encryption keys in this system. In this paper, the values of parameters $a=1.5, b=-1.8, c=1.6, d=0.9$ and initial values $x_0 = 0.14$ and $y_0 = 0.15$ are used. The bifurcation diagram of the Clifford map as shown in Fig. 2 is obtained by taking 66,000 iterations to generate a random sequence of numbers.

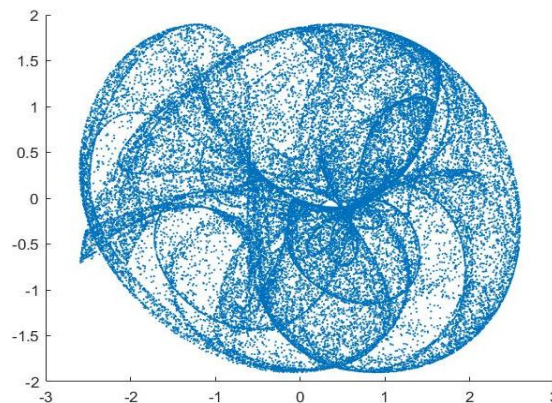


Fig. 2. Bifurcation diagram of Clifford attacker map

2.3 Proposed Encryption Scheme

The proposed encryption scheme is based on the pixel randomization of the image in the Fourier domain. The following is a description of how the Clifford attacker map is implemented in the DRPE scheme:

1. Consider the MN-pixel input image $I(x, y)$.
2. The first random phase mask RPM1 is implanted in the input image, and Fourier processing is done to it.
3. Divide the previous step's resultant image into smaller blocks and transform each one into a vector format.
4. Using the Clifford attacker map, a sequence of random integers is created and sorted in ascending order.
5. Sort the vector you got in step 3 with the vector you got in step 4.
6. Resize the image MN by reshaping the vector produced in step 5.
7. The resulting image is subjected to the second layer of DRPE in which the obtained image is multiplied by a second random phase mask and further Fourier transform is performed, yielding an encrypted image.
8. The decryption process is the inverse of the encryption process in order to recover the original image from the encrypted image.

Along with the keys used in the DRPE scheme, parameters and initial values of the Clifford attacker map work as both encryption and decryption keys for the proposed scheme. The same is also mentioned in Table 2. The whole process of encryption and decryption of the proposed scheme is displayed in Fig. 3.

By implementing the proposed encryption scheme on an input image, we get extra security for an encrypted image in comparison to the DRPE scheme. In the DRPE scheme, an

attacker can retrieve the second random phase mask RPM2. But in the proposed scheme even if the attacker retrieves RPM2 still he won't be able to retrieve the parameters of the Clifford map which works as an extra security level.

3. RESULTS AND DISCUSSION

Three grayscale images of a girl, cameraman, and boat with an image size of 256×256 are used to demonstrate the validity of the proposed technique. MATLAB is used to generate the simulation results. In the simulation, the values of parameters of Clifford attacker map $a=1.5$, $b= -1.8$, $c=1.6$, $d=0.9$ and initial values $x_0 = 0.14$, $y_0 = 0.15$ are used. The validation results of the proposed encryption scheme are shown in Fig. 4. The validation of the encrypted image is carried out using various statistical analyses like a histogram and 3-D plot analysis, correlation distribution analysis, and information entropy. Later, the sensitivity of parameters is discussed followed by basic occlusion and noise attack.

3.1 Histogram and 3-D plot Analysis

To validate the proposed scheme, histogram analysis has been performed on the input images of the girl, cameraman, and boat. For a better encryption algorithm, the histogram of the encrypted image should be different from the histogram of the original image. Fig. (5a-5c) shows the histogram of original images, Fig. (5d-5f) shows a histogram of encrypted images, and Fig. (5g-5i) shows a histogram of decrypted images of a girl, cameraman, and boat respectively. It is clear from Fig. 5 that the histogram of the encrypted image is different from the original image. Pixel values in the histogram of the encrypted image are uniformly distributed i.e., all pixel values have the almost same frequency. Therefore, no statistical information can be obtained through it.

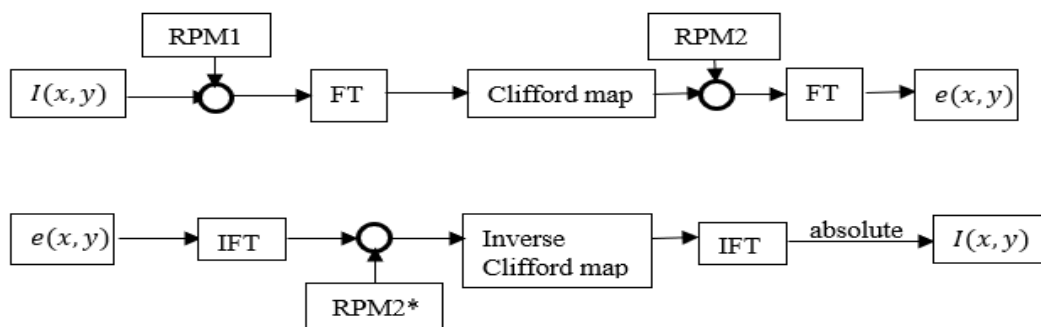


Fig. 3. Encryption and decryption process of the proposed scheme

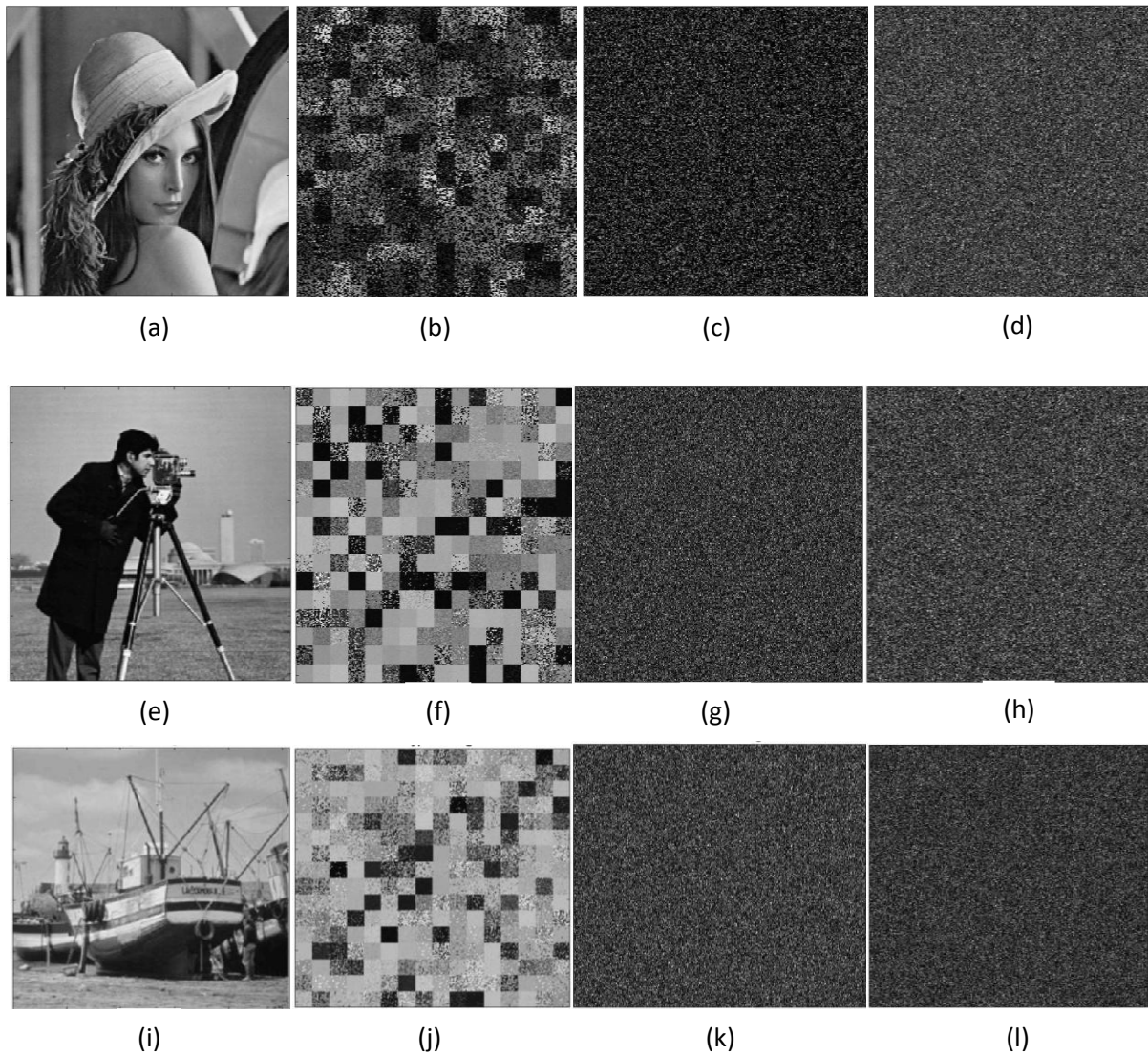
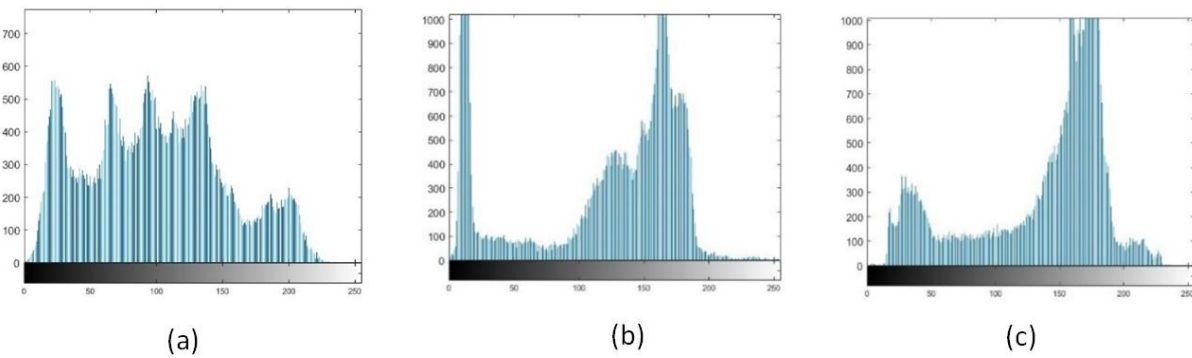


Fig. 4. Scheme validation results; (a,e,i) input images and its encrypted images; (b,f,j) using only Clifford attacker map; (c,g,k) using Double Random Phase Encoding scheme; (d,h,l) using proposed scheme of girl, cameraman and boat respectively



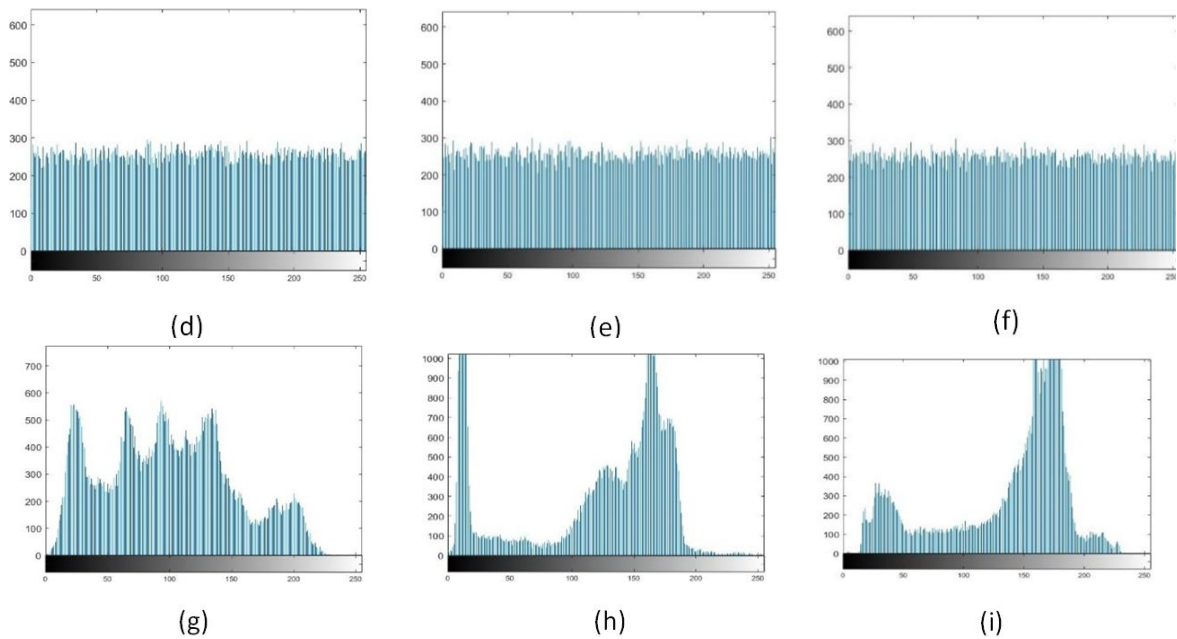
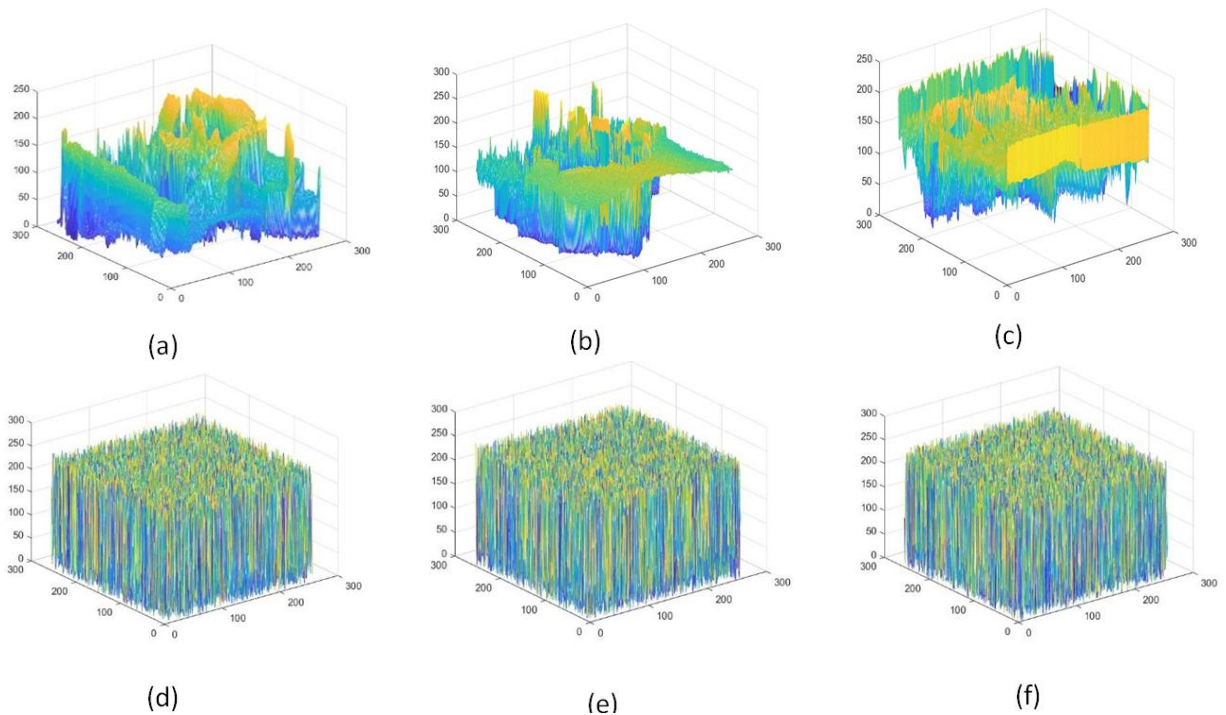


Fig. 5. Histogram of; (a,b,c) input images; (d,e,f) encrypted images; (g,h,i) decrypted images of girl, cameraman and boat respectively

The presented encryption scheme's efficiency may be evaluated using a 3-D visualization of a girl's image. The 3-D plots of the original images are shown in Fig. (6a-6c), encrypted images shown in Fig. (6d-6f), and decrypted images shown in Fig. (6g-6i) of the girl, cameraman, and

boat respectively. Fig. 6 clearly shows that the 3-D plot of the encrypted image is randomly dispersed, however, the 3-D plots of the original image and the decoded image are quite similar, demonstrating the effectiveness of the proposed encryption scheme.



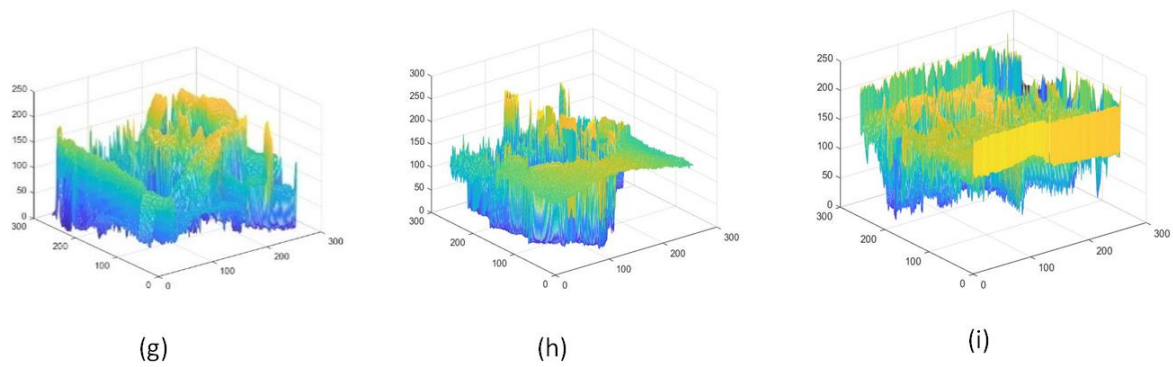


Fig. 6. 3-D plot of; (a,b,c) input images; (d,e,f) encrypted images; (g,h,i) decrypted images of girl, cameraman and boat respectively

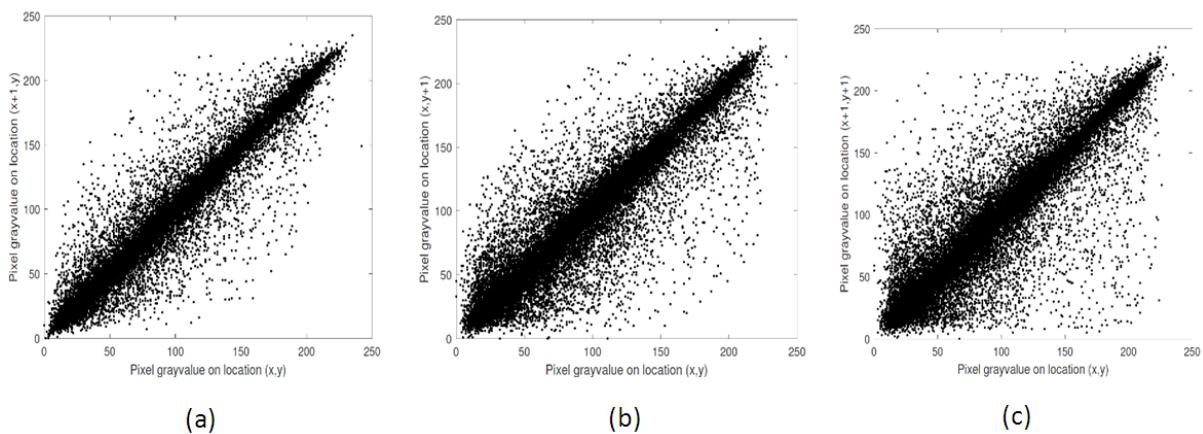
3.2 Correlation Distribution Analysis

Correlation distribution analysis is another approach to demonstrate the efficiency of an encryption scheme. In the horizontal, vertical, and diagonal directions, we plotted 5,000 pairs of adjacent pixels from the original image and its encrypted image of the girl at random. Fig. (7a-7c) shows that neighboring pixels in the input image are substantially connected in all three directions, whereas adjacent pixels in Fig. (7d-7f) of the encrypted image have no correlation. Fig. (7g-7i) displays the correlation distribution of

the retrieved image which is identical to the input image. The comparison clearly shows that the pixels of the encrypted image has lost any correlation, resulting in a random distribution. A similar comparison of correlation distribution plots can be carried out for cameraman and boat images. As shown in Table 1, the correlation coefficient between neighboring pixels from the original image and its encrypted image is computed in the horizontal, vertical, and diagonal directions of the girl, cameraman, and boat images. As a result, the proposed scheme is resistant to statistical attacks.

Table 1. The correlation coefficient between adjacent pixels of the input image and their encrypted images in a horizontal, vertical, and diagonal direction

Image	Type	Horizontal direction	Vertical direction	Diagonal direction
Girl image	Input image	0.9706	0.9436	0.9192
	Encrypted image	-0.0014	0.0097	0.0024
Cameraman image	Input image	0.9431	0.9722	0.9030
	Encrypted image	-0.0067	0.0082	0.0056
Boat image	Input image	0.9554	0.9518	0.9331
	Encrypted image	-0.0074	0.0055	0.0025



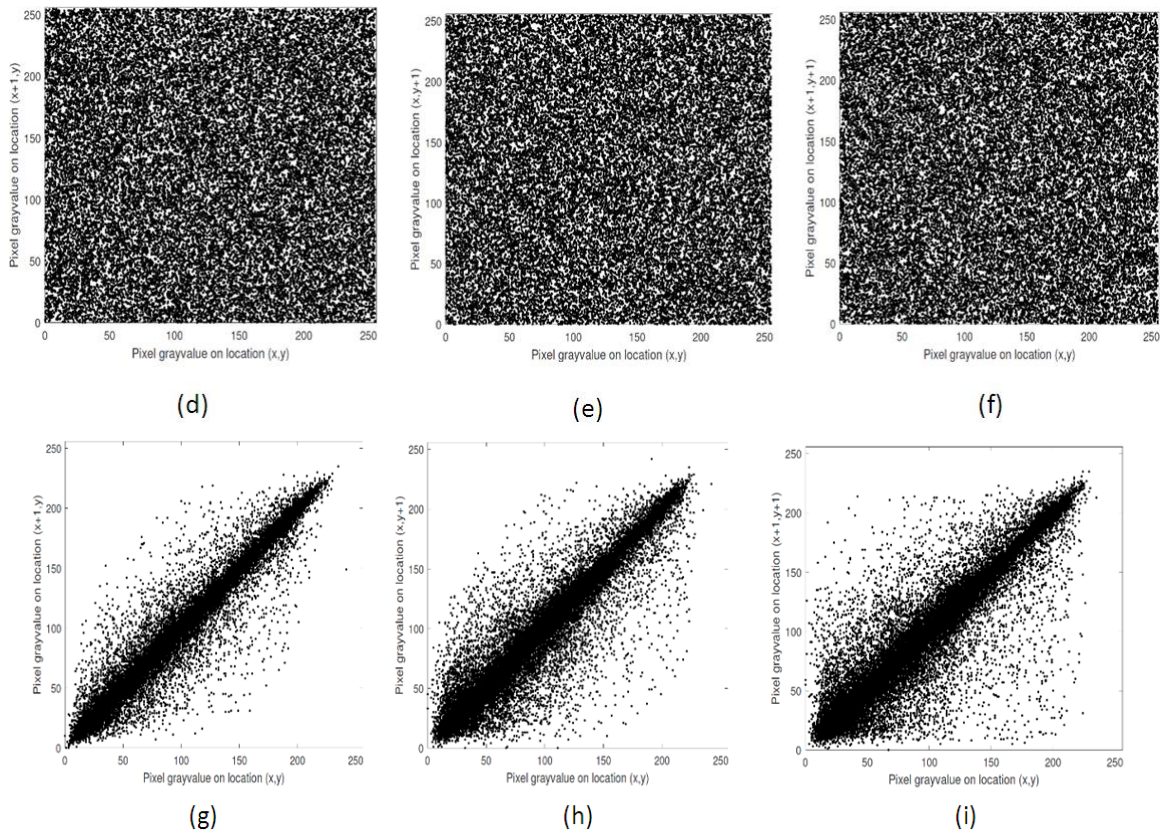


Fig. 7. Correlation distribution plots of pixels of (a-c) input image of girl; (d-f) corresponding encrypted image; (g-i) decrypted image in horizontal, vertical, and diagonal directions respectively

3.3 Information Entropy

The texture of an image can be described using information entropy, which is a statistical measure of unpredictability. The information entropy $H(m)$ of source m , is defined as:

$$H(m) = \sum_{k=1}^{256} p(m_k) \log_2 \frac{1}{p(m_k)}$$

Where $p(m_k)$ is the probability of m_k . The entropy of a grayscale image ranges from 0 to 8. The entropy of a grayscale girl, cameraman and boat images are 7.5784, 7.0583 and 7.1622 while its encrypted image using the proposed scheme has an entropy of 7.9956, 7.9954 and 7.9956. The result shows that the encrypted image's unpredictability and randomness is increased because its entropy value is extremely close to the grayscale image's maximum value.

3.4 Secret-key Sensitivity Analysis

If an image encryption technique has highly sensitive secret keys and has a vast key space to avoid brute force attacks, it is said to be ideal.

The parameters and initial values of the Clifford attacker map, as well as RPM2 of DRPE, serve as secret keys in this scheme. In this scheme, the use of the Clifford map enables the scheme to have six additional secret keys as compared to DRPE to strengthen the proposed scheme. Its strength can be tested by analyzing the sensitivity of the secret key. The results of the sensitivity of parameters and initial values of the Clifford attacker map using the girl image as input image are shown in Fig. 8. From Fig. 8 it is observed that the decrypted image obtained by a slight change in parameter and initial values is completely unrecognizable. The key is sensitive to at least up to fourteen decimal places of each parameter and initial value. Fig. 9 shows the result when we use RPM2 in the decryption process in place of the conjugate of RPM2.

The sensitivity of parameters and initial values of parameters of the Clifford attacker map is also demonstrated against variation in the parameters and initial values of this map in terms of correlation coefficient (CC) plots. Fig. 10 explored the correlation coefficient between the

original and retrieved image of the girl while slight (10a) deviation in the parameter a, (10b) deviation in b, (10c) deviation in c, (10d) deviation in d, (10e) deviation in x_0 , (10f) deviation in y_0 up to order 10^{-15} . It is clear from Fig. 10 that the value of CC=1 was obtained only for the zero deviation which means the correct

value of the parameter. CC is very close to zero even for a slight deviation in parameter. The extremely sensitive nature of the parameters of the Clifford attacker map demonstrates the robustness of the proposed scheme. Similar sensitivity analysis can also be done using cameraman and boat images.

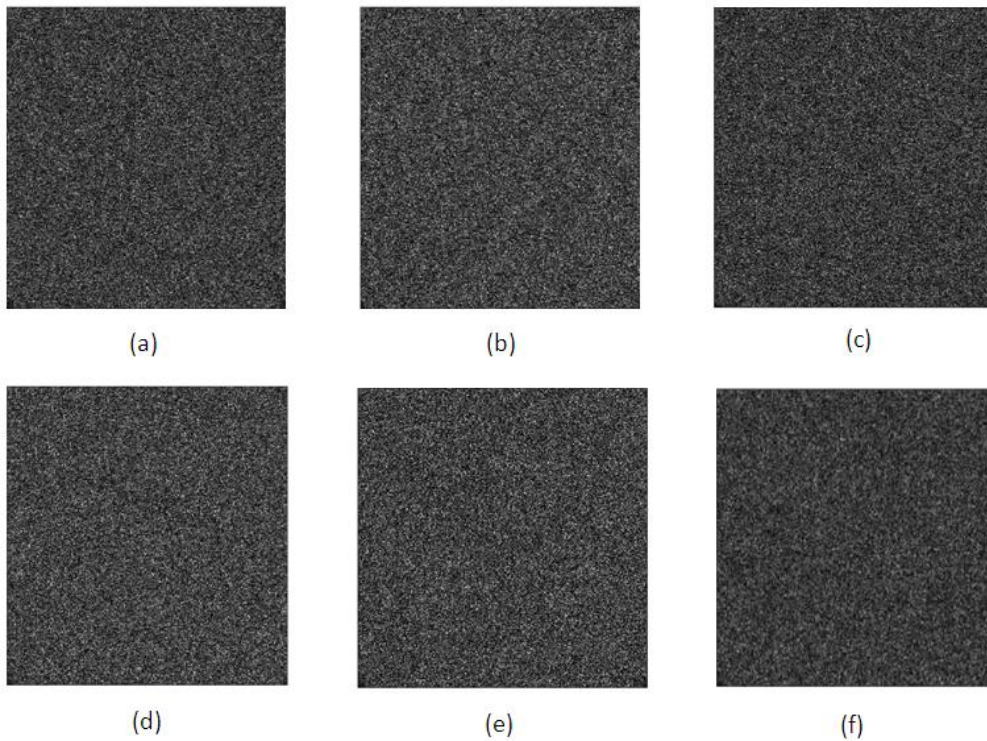


Fig. 8. Decrypted image of girl; (a) incorrect parameter $a=1.499999999999999$ is used instead of $a=1.5$; (b) incorrect parameter $b=-1.799999999999999$ is used instead of $b=-1.8$; (c) incorrect parameter $c=1.599999999999999$ is used instead of $c=1.6$; (d) incorrect parameter $d=0.899999999999999$ is used instead of $d=0.9$; (e) incorrect initial value $x_0=0.139999999999999$ is used instead of $x_0=0.14$; (f) incorrect initial value $y_0=0.149999999999999$ is used instead of $y_0=0.15$

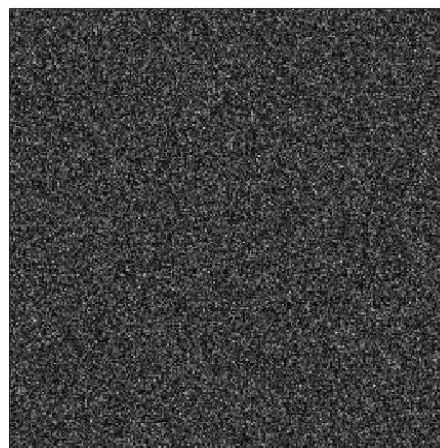


Fig. 9. Decrypted image using RPM2 in place of the conjugate of RPM2

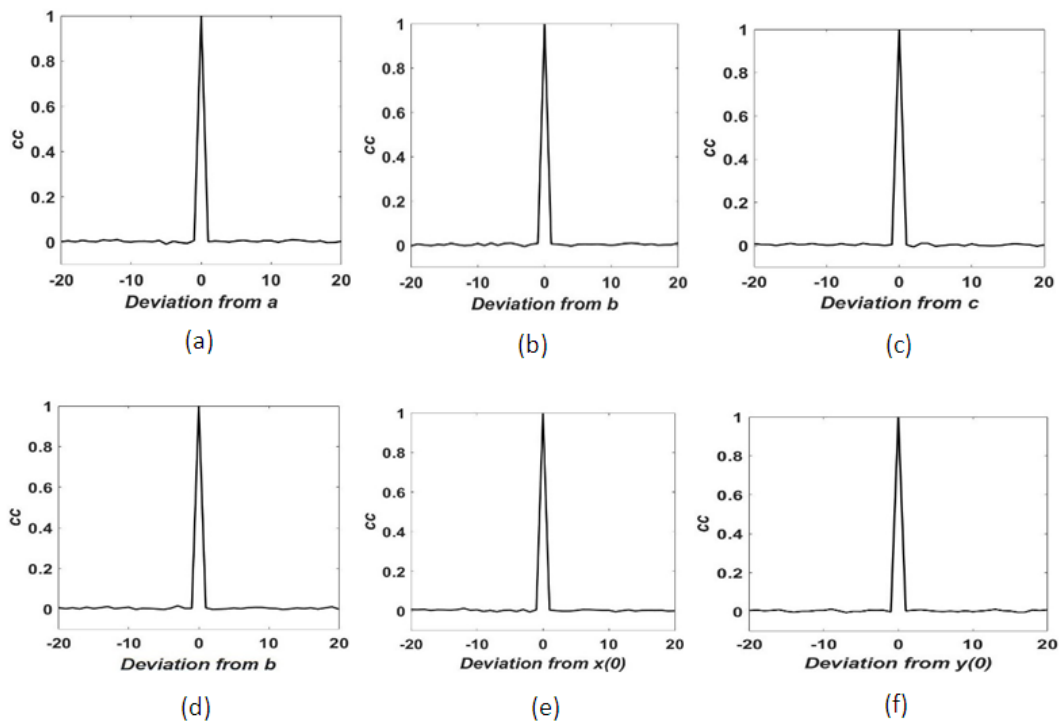


Fig. 10. Correlation coefficient versus incorrect deviation value of the parameters a, b, c, d and initial value x_0, y_0 of Clifford attacker map

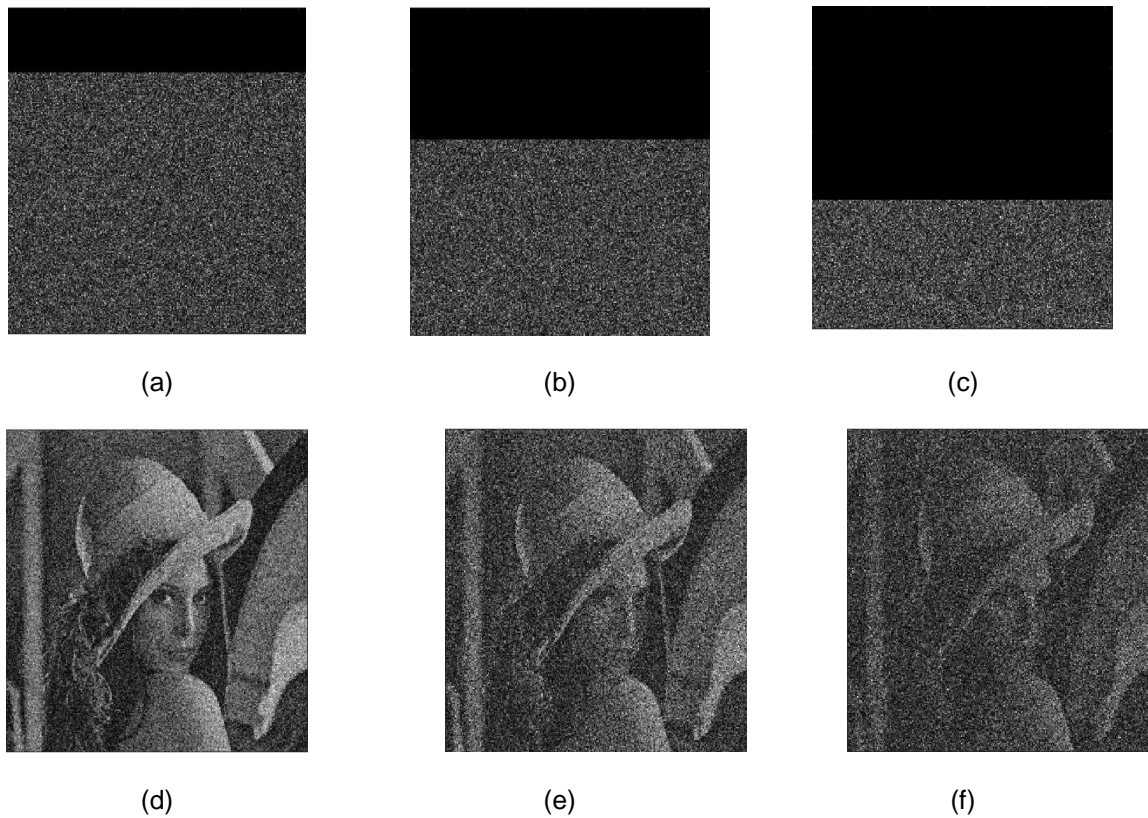


Fig. 11. Encrypted image with occluded part; (a-c) 20%, 40% and 60%; (d-f) their corresponding decrypted image



Fig. 12. Decrypted image with noise strength (a) $k=3$; (b) $k=6$; (c) $k=9$

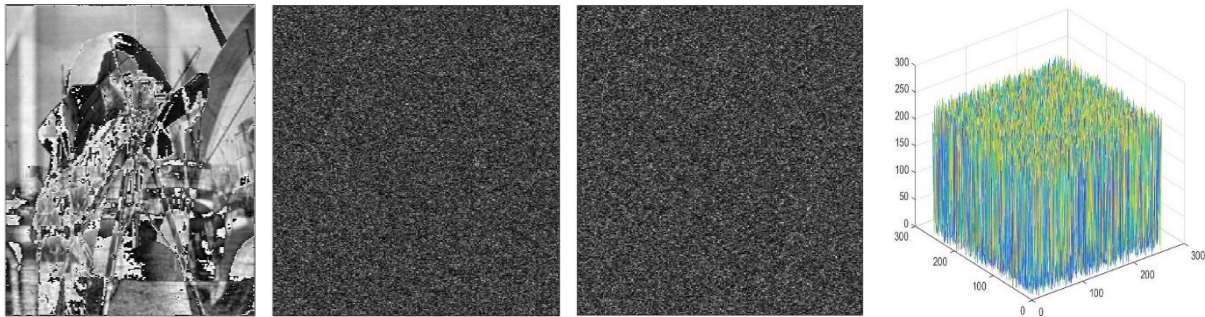


Fig. 13. (a) Combined image of girl, cameraman and boat images $A_1 + A_2 + A_3$, (b) corresponding encrypted image $f(A_1 + A_2 + A_3)$ (c) difference of $f(A_1 + A_2 + A_3)$ and $f(A_1) + f(A_2) + f(A_3)$ and (d) 3D plot of difference of $f(A_1 + A_2 + A_3)$ and $f(A_1) + f(A_2) + f(A_3)$.

Table 2. Comparison of the proposed scheme with existing schemes

	Elshamy et al. [15]	Sharma et al. [16]	Refriger and Javidi [3]	Clifford System-Based scheme	Proposed scheme
Number of keys	RPM+ additional layer using Arnold's cat map	RPM+ 9 keys	RPM	6 keys	RPM + 2 initial values and 4 parameters of Clifford attacker map
Permutation procedure employed	Yes	Yes	No	Yes	Yes
Applied strategy	Digital or optical	Digital or optical	Digital or optical	Optical	Digital or optical
The correlation coefficient between input and encrypted image	-0.0011	Not evaluated	-0.0064	-0.0516	-0.0050
Entropy	Not evaluated	7.7460	7.9853	7.5784	7.9956
MSE	8.91×10^{-28}	Not evaluated	3.1334×10^{-27}	0	2.9808×10^{-27}
PSNR	318	10.2918	313	∞	314

3.5 Occlusion Attack Analysis

On the encrypted image of the girl, an occlusion attack is carried out by obscuring 20%, 40%, and 60% of the encrypted image as shown in Fig. (11a-11c) respectively. Then, using the proposed decryption procedure, this occluded image is decoded. As can be seen in Fig. (11d-11f), the quality of the encrypted image degrades as the area of the occluded component grows larger, although the image is still recognizable as up to 60% occluded. Similarly, outputs of the occlusion attack were obtained from cameraman and boat images. As a result, the technique can withstand a broader spectrum of occlusion attacks.

3.6 Noise Attack Analysis

In this subsection, the proposed technique is tested to check its ability to endure the noise attack. The noise of strength 'k' is added to the encrypted image E_n according to the formula:

$$E_0 = E_n(1 + kG)$$

Where E_0 is the noise-affected encrypted image and G is the Gaussian noise with mean zero and variance 1. The retrieved images of the girl are shown in Fig. (12a-12c) when the encrypted image is affected by noise with increasing noise strength k . The clarity of the decrypted image has reduced, but it is still discernible.

3.7 Linearity Analysis

Crypto scheme f is said to be linear if

$$f(A_1 + A_2 + A_3 + \dots + A_n) = f(A_1) + f(A_2) + \dots + f(A_n)$$

where A_i denote input image and $f(A_i)$ corresponding encrypted image.

We analyze the linearity of proposed scheme by considering three input images of girl, cameraman and boat images denoted by A_1, A_2, A_3 . Then $A_1 + A_2 + A_3$ shown in Figure 13(a) is encrypted as $f(A_1 + A_2 + A_3)$ shown in Figure 13(b). Non-linear behavior of the scheme can be visible from the difference of $f(A_1 + A_2 + A_3)$ and $f(A_1) + f(A_2) + f(A_3)$ in figure 13(c) and its 3D plot in figure 13(d).

4. CONCLUSION

The current paper introduces a novel grayscale image encrypting technique. For pixel scrambling in the Fourier domain, the approach employs the

Clifford attacker map. Two random phase masks RPM1 and RPM2 are used, one in the spatial domain and the other in the Fourier Domain. Through simulation in MATLAB, the proposed scheme is validated on images of a girl, cameraman, and boat as shown in Fig. 4. For a good encryption scheme, the value of the information entropy of the encrypted image should be high while the correlation coefficient and mean square error value between the original and encrypted image should be low. A comparison with different algorithms was conducted which shows the value of information entropy increases from 7.9853 in DRPE to 7.9956 in the proposed scheme whereas the correlation coefficient and mean square error between the original and encrypted image decreases from -0.0064 in DRPE to -0.0050 in the proposed scheme and 3.1334×10^{-27} in DRPE to 2.9808×10^{-27} in the proposed scheme respectively. Its efficacy is assessed using statistical methods like histogram, 3-D plot, and correlation distribution analysis which shows more randomness occurs in encrypted images which are obtained using the proposed scheme. Sensitivity analysis also revealed that the new technique is quite sensitive to Clifford map parameters. As a result, these parameters work as extra encryption keys. Hence security level of the original image increases. Due to its nonlinear behavior, known plaintext and chosen plaintext attacks are not applicable. The scheme also demonstrates its endurance to occlusion and noise attacks.

COMPETING INTERESTS

Authors have declared that no competing interests exist.

REFERENCES

1. Daemen J, Rijmen V. Reijndael: the advanced encryption standard. Dr. Dobbs J Softw Tool Prof Programmer. 2001;26(3):137-9.
2. Davis R. The data encryption standard in perspective. IEEE Commun Soc Mag. 1978;16(6):5-9.
3. Refregier P, Javidi B. Optical image encryption based on input plane and Fourier plane random encoding. Opt Lett. 1995;20(7):767-9.
4. Javidi B, Sergent A, Zhang G, Guibert L. Fault tolerance properties of a double phase encoding encryption technique. Opt Eng. 1997;36(4):992-8.

5. Goudail F, Bollaro F, Javidi B, Réfrégier P. Influence of a perturbation in a double phase-encoding system. *J Opt Soc Am A*. 1998;15(10):2629-38.
6. Unnikrishnan G, Joseph J, Singh K. Optical encryption by double-random phase encoding in the fractional fourier domain. *Opt Lett*. 2000;25(12):887-9.
7. Situ G, Zhang J. Double random-phase encoding in the Fresnel domain. *Opt Lett*. 2004;29(14):1584-6.
8. Chen L, Zhao D. Optical image encryption with Hartley transforms. *Opt Lett*. 2006;31(23):3438-40.
9. Nishchal NK, Joseph J, Singh K. Fully phase encryption using fractional fourier transform. *Opt Eng*. 2003;42(6):1583-8.
10. Peng X, Zhang P, Wei H, Yu B. Known-plaintext attack on optical encryption based on double random phase keys. *Opt Lett*. 2006;31(8):1044-6.
11. Carnicer A, Montes-Usategui M, Arcos S, Juvells I. Vulnerability to chosen-ciphertext attacks of optical encryption schemes based on double random phase keys. *Opt Lett*. 2005;30(13):1644-6.
12. Peng X, Wei H, Zhang P. Chosen-plaintext attack on lensless double-random phase encoding in the fresnel domain. *Opt Lett*. 2006;31(22):3261-3.
13. Sharma N, Saini I, Yadav A, Singh P. Phase image encryption based on 3D Lorenz chaotic system and double random phase encoding. *3D Res*. 2017;8(4):39.
14. Elshamy AM, Rashed ANZ, Mohamed AEA, Faragalla OS, Mu Y, Alshebeili SA et al. Optical image encryption based on chaotic Baker map and double random phase encoding. *J Lightwave Technol*. 2013;31(15):2533-9.
15. Elshamy AM, El-Samie A, Fathi E, Faragallah OS, Elshamy EM, El-sayed HS. El-zoghdy, S., Rashed, A.N., Mohamed, A.E.N.A. and Alhamad, A.Q. *Opt Quantum Electron*. 2016. Optical image cryptosystem using double random phase encoding and arnold's cat map;48(3):1-18.
16. Sharma N, Saini I, Yadav A, Singh P. Phase-image encryption based on 3d-lorenz chaotic system and double random phase encoding. *3D Res*. 2017;8(4):1-17.
17. Singh N, Sinha A. Optical image encryption using fractional fourier transform and chaos. *Opt Lasers Eng*. 2008;46(2):117-23.
18. Rakheja P, Singh P, Vig R, Kumar R. Double image encryption scheme for iris template protection using 3D Lorenz system and modified equal modulus decomposition in hybrid transform domain. *J Mod Opt Apr*. 2020;67(7):592-605.
19. Tobria A, Yadav S, Singh P. Cryptosystem based on triple random phase encoding with chaotic Henon map. In book. *Proceedings of the international conference on data science and applications*; 2020. p. 73-84.
20. Rakheja P, Vig R, Singh P. Double image encryption using 3D Lorenz chaotic system, 2D non-separable linear canonical transform and QR decomposition. *Opt Quantum Electron*. 2020;52(2):103.
21. Yadav S, Singh P. A novel chaotic Umbrella map and its application to image encryption. *Opt Quantum Electron*. 2022;54.
22. Giesl J, Behal L, Viecek K. Improving chaos image encryption speed. *International journal of future generation communication and networking*. 2009;2(3):23-36.
23. Kanafchian M, Fathi-Vajargah B. A novel image encryption scheme based on Clifford attractor and noisy logistic map for secure transferring images in navy. *Int J e-Navigation Marit Econ*. 2017;6: 53-63.

© 2022 Kalra et al.; This is an Open Access article distributed under the terms of the Creative Commons Attribution License (<http://creativecommons.org/licenses/by/4.0>), which permits unrestricted use, distribution, and reproduction in any medium, provided the original work is properly cited.

Peer-review history:

The peer review history for this paper can be accessed here:

<https://www.sdiarticle5.com/review-history/93025>